INTERNATIONAL ATOMIC ENERGY AGENCY
UNITED NATIONS EDUCATIONAL, SCIENTIFIC AND CULTURAL ORGANIZATION
INTERNATIONAL CENTRE FOR THEORETICAL PHYSICS
I.C.T.P., P.O. BOX 586, 34100 TRIESTE, ITALY, CABLE: CENTRATOM TRIESTE

SMR.769 - 9

**WORKSHOP ON
"NON-LINEAR ELECTROMAGNETIC INTERACTIONS
IN SEMICONDUCTORS"**

1 - 10 AUGUST 1994

"Logic gates and optical switching with vertical cavity surface emitting lasers"

F. PRATI
Dipartimento di Fisica
Universita' di Milano
Via Celoria 16
20133 Milano
Italy

These are preliminary lecture notes, intended only for distribution to participants

MAIN BUILDING STRADA COSTIERA, 11 TEL. 22401 TELEFAX 224163 TELEX 460392 ADRIATICO GUEST HOUSE VIA GRIGNANO, 9 TEL. 224241 TELEFAX 224531 TELEX 460449
MICROPROCESSOR LAB. VIA BEIRUT, 31 TEL. 224471 TELEFAX 224600 TELEX 460392 GALILEO GUEST HOUSE VIA BEIRUT, 7 TEL. 22401 TELEFAX 2240310 TELEX 460392

Logic gates and optical switching with vertical cavity surface emitting lasers

F. Prati, M. Travagnin and L.A. Lugiato
Dipartimento di Fisica dell' Università di Milano
via Celoria 16, 20133 Milano, Italy
Tel: +39-2-2392470, Fax: +39-2-2392712

Abstract

We show that an index–guided vertical cavity surface emitting laser with square-shaped active region can operate as a bistable laser with the two Gauss-Hermite modes TEM_{10} and TEM_{01} . We study numerically optical switching from one mode to the other upon injection of an appropriate external field, and we demonstrate the possibility of using the laser as a logic gate of the NOR, OR, NOT type.

I. INTRODUCTION

The last decade witnessed the development of the field of Transverse Nonlinear Optics [1, 2], which studies the phenomena of spontaneous pattern formation and transformation which occur in the structure of the electric field in the planes orthogonal to the direction of propagation, when the radiation interacts with nonlinear optical media. The fast time evolution in optical systems makes Transverse Nonlinear Optics potentially useful for applications to information processing.

In this perspective the phenomenon of "spatial multistability" is of great relevance [3,4]. It consists in the capability, displayed by several kinds of lasers, of emitting beams with different spatial configurations, under the same parametric conditions. This situation is quite different from standard optical bistability, where the stable states differ only for the emitted power. On the contrary, in spatial multistability the total emitted power for the different stable states is usually almost the same. The different states can be distinguished only on the basis of the field spatial configuration.

The simplest case of multistability is represented by bistability of the two lowest order doughnut modes, which has been experimentally demonstrated in a He–Ne laser [5]. Application to optical switching has been reported in [6], where it has been shown that the bistable laser can switch from one to the other doughnut mode by injection of an external field whose intensity is very small, compared with that of the slave laser.

Our first aim, when we started working on this research, was to simply extend the results of [6] to a class of lasers such as VCSELs (vertical cavity surface emitting lasers) [7] which are much more suitable for practical applications, because of their small dimensions and fast response. Actually, it has been recently demonstrated that the transverse modes of these lasers can be with good approximation described as Gauss–Hermite modes [8].

Yet, even the crudest attempt to model transverse effects in VCSELs, which consists in a rate equation model which takes into account the band structure of the energy levels by means of the introduction of the phenomenological linewidth enhancement factor α [9], showed that the behaviour of VCSELs is very different from that of gas lasers, which can be described by the standard Maxwell–Bloch equations for two-level atoms.

It is known that in Class–A lasers, and in Class–B lasers under conditions of resonance between the gain line and the cavity, the doughnut modes are always stable for every choice of the parameters [11]. In the simple model of [10] VCSELs turn out to be mathematically equivalent to Class–B lasers with a normalized atomic detuning equal to α. Since α ranges from 3 to 6 [9], the correspondence is with Class–B lasers with large atomic detuning. For this kind of lasers the doughnut modes are unstable almost everywhere and the most common situation is that in which the laser develops undamped oscillations. However, for $\alpha > 1$ a stability domain for modes TEM_{10} and TEM_{01} exists in the parameter space [10].

The latter result was quite surprising, because previously it was believed that modes TEM_{10} or TEM_{01} could be stabilized only by a breaking of the cylindrical symmetry [12] which favours one of the two. Therefore bistability between these two modes was excluded a priori. In VCSELs, instead, it is possible to obtain bistability between TEM_{10} and TEM_{01} by considering an active region of square instead of circular section [10].

From the point of view of applications this kind of bistability is even preferable to bistability between doughnut modes, because it allows to obtain switching using Gaussian-shaped control beams, and to realize logic gates.

In Sec. 2 we briefly summarize the theoretical results obtained in [10]. Numerical simulations of optical switching of modes TEM_{10} and TEM_{01} are presented in Sec. 3, where the essential role of detuning between the injecting laser and the slave laser is also discussed. In Sec. 4 we suggest a scheme for the realization of NOR, OR and NOT gates based on the bistable VCSEL. Sec. 5 is devoted to the concluding remarks.

II. THE MODEL

We consider a weakly index-guided cylindrical VCSEL. The diameter of a circular transverse section is d, L_A is the thickness of the active region and L is the length of the cavity, considering the penetration in the Bragg reflectors (Fig. 1). We adopt cylindrical coordinates (r, φ, z) with the z-axis coincident with the optical axis of the laser and assume that the refractive index inside the material has a parabolic radial profile

$$n^2(r) = n^2(0)\left(1 - \frac{r^2}{h^2}\right) \tag{2.1}$$

with $h \gg d$, in such a way that the variation of the refractive index from the axis to the edge is small.

This kind of resonator is able to sustain Gaussian modes whose waist w_0 is related to h and to the wavelength λ by the equation [10]

$$w_0 = \sqrt{\frac{\lambda h}{\pi}} \,. \tag{2.2}$$

Thus, h plays the same role as the Rayleigh length in an open resonator with spherical mirrors.

The eigenmode of order p, l, with $p = 1, 2, \ldots$ and $l = \pm 1, \pm 2, \ldots$ is described by the Gauss-Laguerre function [10]

$$\mathcal{A}_{pl}(\rho, \varphi, z) = A_{pl}(\rho, \varphi) e^{-i(2p+|l|+1)z/h} \,, \tag{2.3a}$$

$$A_{pl}(\rho, \varphi) = \left[\frac{2}{\pi}\right]^{1/2} \left[\frac{p!}{(p+|l|)!}\right]^{1/2} (2\rho^2)^{|l|/2} L_p^{|l|}(2\rho^2) e^{-\rho^2} \, e^{il\varphi} \,, \tag{2.3b}$$

where $\rho = r/w_0$. The modes gather in frequency degenerate families of order $q = 2p + |l|$, composed by $q + 1$ modes.

In the mean field and single longitudinal mode approximations we assume that the single-pass gain and phase shift for the transverse modes with the same longitudinal index are small and the reflectivity of the Bragg reflectors is close to 1. Then, the dependence on the longitudinal coordinate z can be neglected and the forward and backward field turn out to be equal. We expand the slowly varying envelope $F(\rho, \varphi)$ of the electric field in terms of the modes $A_{pl}(\rho, \varphi)$

$$F(\rho, \varphi, \tau) = \sum_{pl} A_{pl}(\rho, \varphi) f_{pl}(\tau) \tag{2.4}$$

The complex mode amplitudes f_{pl} obey the equations [10]

$$\frac{df_{pl}}{d\tau} = -\tilde{k} \left[(1 + \mathrm{i}a_{pl}) f_{pl} - 2Ck(1 - \mathrm{i}\alpha) \int_0^{2\pi} d\varphi \int_0^{\infty} d\rho\rho \; A^*_{pl} \, D \, F \right] \tag{2.5}$$

and they are coupled to the normalized carrier density D through the rate equation

$$\frac{\partial D}{\partial \tau} = -D(1 + |F|^2) + \chi_V \ , \tag{2.6}$$

in which we neglected both grating effects and diffusion. Time τ is measured in units of the recombination time τ_r. Accordingly, $\tilde{k} = k\tau_r$ is the adimensional cavity linewidth, where

$$k = \frac{c |\ln \sqrt{R_1 R_2}|}{2n(0)L} \ ; \tag{2.7}$$

R_1 and R_2 are the reflectivities of the two Bragg reflectors and $n(0)$ is the refractive index on the laser axis.

The other parameters of Eqs. (2.5) and (2.6) are the normalized gain coefficient $2C$, the linewidth enhancement factor α and the transverse frequency spacing between mode (p, l) and the fundamental Gaussian mode

$$a_{pl} = \frac{\omega_{pl} - \omega_{00}}{k} \ . \tag{2.8}$$

In terms of the usual semiconductor parameters the quantities $2C$ and D are written as

$$2C = \frac{aN_0 L_A}{|\ln \sqrt{R_1 R_2}|} \left(\frac{I}{I_0} - 1 \right) \ , \tag{2.9a}$$

$$D = \frac{N/N_0 - 1}{I/I_0 - 1} \ , \tag{2.9b}$$

with

$$I_0 = \frac{q_e V N_0}{\tau_r} \ . \tag{2.9c}$$

Here a is the phenomenological gain coefficient, N is the carrier density, N_0 is its transparency value, q_e is the electron charge, and V is the volume of the active region. Typical values for the physical quantities involved in the definitions are $a = 3 \times 10^{-16}$ cm^2, $N_0 = 3 \times 10^{18}$ cm^{-3}, $V = 4 \times 10^{-12}$ cm^3, $\tau_r = 0.2 \div 1 \times 10^{-9}$ sec, $L_A = 4 \times 10^{-6}$ cm, and $R_1, R_2 > 0.99$.

The function χ_V describes the transverse shape of the active region. Let us consider, for instance, the case in which a square window of normalized size $\psi = l/w_0$ (Fig. 1) is placed on one of the surfaces of the laser. The square geometry suggests using cartesian coordinates x and y (normalized to w_0) and we write

$$\chi_V(x,y) = \begin{cases} 1 & |x|,\ |y| \le \psi/2\ , \\ 0 & |x|,\ |y| > \psi/2\ . \end{cases} \tag{2.10}$$

We are interested in the case that only the two modes of family $q = 1$ are active. This condition can be obtained by putting a small absorbing or metallic dot on the laser axis in order to suppress the fundamental Gaussian mode TEM_{00} and by adjusting the size of the square window in such a way that the modes belonging to families with $q > 1$ are below threshold.

The linear stability analysis shows that the only stable states of the laser under these conditions can be (according to the value of the pump parameter) the two doughnut modes $A_{0\pm1}$ or the two TEM_{10} and TEM_{01} modes placed on the diagonals of the square [10]

$$B_1(x,y) = \frac{2}{\sqrt{\pi}}(x+y)\exp(-x^2-y^2) \qquad (TEM_{10})\ , \tag{2.11a}$$

$$B_2(x,y) = \frac{2}{\sqrt{\pi}}(x-y)\exp(-x^2-y^2) \qquad (TEM_{01})\ . \tag{2.11b}$$

The transverse intensity distributions of the doughnut modes and of modes TEM_{10} and TEM_{01} are shown in Figs. 2.

We introduce the pump parameter β, defined as

$$\beta = \frac{2C}{2C_{thr}} - 1\ , \tag{2.12}$$

where $2C_{thr}$ is the threshold value for laser emission, which depends only on ψ

$$2C_{thr} = \left[\frac{2}{\pi} J_0\left(\frac{\psi}{\sqrt{2}}\right) J_2\left(\frac{\psi}{\sqrt{2}}\right)\right]^{-1} \tag{2.13}$$

with

$$J_n(z) = \int_{-z}^{z} dx\, x^n\, e^{-x^2}\ . \tag{2.14}$$

Once fixed α, $\tilde{k}$ and ψ, the boundaries of the stability domains for the two kinds of stationary solutions are assigned by the following critical values of β

$$\beta_1 = \frac{1}{\tilde{k}\alpha^2} \tag{2.15}$$

$$\beta_\pm = \frac{1}{2\tilde{k}} \frac{H(1+\alpha^2) + 2(1-2H) \pm \sqrt{H^2(1+\alpha^2)^2 - 4\alpha^2(1-2H)^2}}{(1-H)^2(1+\alpha^2)} \tag{2.16}$$

with

$$H(\psi) = \frac{J_0(\psi)J_4(\psi) - J_2(\psi)^2}{J_0(\psi)J_4(\psi) + 3J_2(\psi)^2} \tag{2.17}$$

By increasing β we meet the following sequence of stationary and dynamical regimes:

a) $0 < \beta < \beta_1$: the two doughnut modes are stable,

b) $\beta_1 < \beta < \beta_-$: the two doughnut modes beat at frequency $\omega_1 = (\tau_r \alpha)^{-1}$,

c) $\beta_- < \beta < \beta_+$: modes TEM_{10} and TEM_{01} are stable,

d) $\beta > \beta_+$: modes TEM_{10} and TEM_{01} beat at frequency

$$\omega_2 = \frac{1}{\tau_r} \frac{\left[-2(1-2H)^2 + H^2(1+\alpha^2) + H\sqrt{H^2(1+\alpha^2)^2 - 4\alpha^2(1-2H)^2}\right]^{1/2}}{\sqrt{2}(1-H)} . \tag{2.18}$$

Fig. 3 shows the stability domains of the doughnut modes and of modes TEM_{10} and TEM_{01} in the (ψ, β) plane for $\alpha = 4$ and $\tilde{k} = 10$. The last value is obtained assuming $R_1 \cdot R_2 = 0.996$, $n(0)L = 6$ μm and $\tau_r = 0.2 \times 10^{-9}$ s.

It is worth noting that the width of the two bistability domains is inversely proportional to $\tilde{k} = k\tau_r$: in order to have significant bistability domains above threshold, the cavity linewidth k must not be too much larger than the decay rate of carriers τ_r^{-1}. This requires very high mirror reflectivity ($R > 0.995$).

III. OPTICAL SWITCHING OF MODES TEM_{10} AND TEM_{01}

Since the bistability domain of doughnut modes is very small, in the following we will consider only the case in which the two bistable states of the VCSELs are modes TEM_{10} and TEM_{01} . In this section we will investigate the conditions for switching from one to the other mode by means of an injected signal.

Let us assume that the VCSEL is emitting mode TEM_{10} (B_1), and we want to cause switching to mode TEM_{01} (B_2). We assume that the injected field is a gaussian (both in time and in space) pulse of temporal width σ and spatial width $\eta = w_{inj}/w_0$, and centered at a point (x_0, y_0) in the transverse plane, close to one of the two intensity peaks of mode TEM_{01} :

$$F_{inj}(x,y,\tau) = \sqrt{P}\ \left[\frac{2}{\pi}\right]^{1/2} \frac{1}{\eta} \exp\left[-\frac{(x-x_0)^2+(y-y_0)^2}{\eta^2}\right] \left[\frac{2}{\pi}\right]^{1/4} \exp\left[-\frac{(\tau-\tau_0)^2}{\sigma^2}\right] . \quad (3.1)$$

The total injected energy is given by

$$E = \tau_r \int_{-\infty}^{\infty} dx \int_{-\infty}^{\infty} dy \int_{-\infty}^{\infty} d\tau\ F_{inj}^2 = \sigma \tau_r P \quad (3.2)$$

where P is the maximum normalized injected power. We call y_1 and y_2 the projections onto modes TEM_{10} (B_1) and TEM_{01} (B_2), respectively. Using Eqs. (2.11), we obtain

$$y_1 = \sqrt{P}\, 2\sqrt{\pi} \left[\frac{2}{\pi}\right]^{3/4} \exp\left[-\frac{(\tau-\tau_0)^2}{\sigma^2}\right] \frac{\eta}{(1+\eta^2)^2} \exp\left[-\frac{x_0^2+y_0^2}{1+\eta^2}\right] (x_0+y_0) \quad (3.3a)$$

$$y_2 = \sqrt{P}\, 2\sqrt{\pi} \left[\frac{2}{\pi}\right]^{3/4} \exp\left[-\frac{(\tau-\tau_0)^2}{\sigma^2}\right] \frac{\eta}{(1+\eta^2)^2} \exp\left[-\frac{x_0^2+y_0^2}{1+\eta^2}\right] (x_0-y_0) \quad (3.3b)$$

The parameters η, x_0 and y_0 are chosen in such a way that the projection onto mode TEM_{01} is maximum and that onto mode TEM_{10} is zero; this occurs when $x_0 = -y_0 = \sqrt{3/8}$ and $\eta = 1/\sqrt{2}$.

The dynamical equations of the laser with injected signal are then

$$\frac{dg_1}{d\tau} = -\mathrm{i}\Delta\omega g_1 - \bar{k}(1-\mathrm{i}\alpha)\left[g_1 - 2C\int_{-\infty}^{\infty} dx \int_{-\infty}^{\infty} dy\ B_1\, D\, F\right] \quad (3.4a)$$

$$\frac{dg_2}{d\tau} = -\mathrm{i}\Delta\omega g_2 - \bar{k}(1-\mathrm{i}\alpha)\left[g_2 - 2C\int_{-\infty}^{\infty} dx \int_{-\infty}^{\infty} dy\ B_2\, D\, F\right] + \bar{k} y_2(\tau) \quad (3.4b)$$

$$\frac{\partial D}{\partial \tau} = -\left[D(1+|F|^2) - \chi v\right] \quad (3.4c)$$

with

$$F(x,y,\tau) = B_1(x,y)g_1(\tau) + B_2(x,y)g_2(\tau) \quad (3.5)$$

and

$$y_2(\tau) \simeq 0.59\sqrt{P} \exp\left[-\frac{(\tau-\tau_0)^2}{\sigma^2}\right] . \quad (3.6)$$

The parameter $\Delta\omega$ represents the detuning between the injected and the cavity field in units of τ_r^{-1}, and it plays a crucial role in the switching process. If $\Delta\omega$ is too small, switching turns out to be very sensitive to the injection parameters, namely the amplitude and duration of the injected pulse and its phase relative to the cavity field. Conversely, if $\Delta\omega$ is too large, switching becomes insensitive to the pulse duration and phase, but its threshold becomes very high.

Let us first examine the laser behaviour in the case $\Delta\omega = 0$. If the pulse is long and strong enough to cause an energy transfer that brings the laser to the upper unstable region of Fig. 3 the two competitive modes develop oscillations (Fig. 4), and it becomes impossible to control which of the two will finally dominate. These oscillations can be avoided only by reducing the energy transfer to the system to the minimum value which is necessary to obtain switching; in principle this can be accomplished by injecting for a short time a pulse of low power. Unfortunately our simulation shows that in this case it becomes necessary to control the pulse phase. Fig. 5 and Fig. 6 show the evolution of the two amplitudes g_1 and g_2 for injected pulses with the same amplitude and duration, but different phases: switching occurs in the case of Fig. 5 and it does not in the case of Fig. 6.

The introduction of a small detuning $\Delta\omega$ between the injected pulse and the cavity field has both positive consequences of reducing the energy transfer to the system and eliminating the switching dependence on the phase. As one can see in Fig. 7, in the complex plane the effect of the detuned injected field is causing a relative rotation of the amplitudes g_1 and g_2. To erase completely any influence on the switching process from the initial relative phase it is necessary that the pulse is long enough that during injection g_2 rotates at least 5-10 times around g_1 (Fig. 7); since the number of rotations can be roughly estimated to be $2\sigma\,\Delta\omega/2\pi$, the minimum pulse length is given by $\sigma \simeq 5 - 10\,\pi/\Delta\omega$. An unavoidable drawback is that the minimum power which has to be injected to have switching increases, as shown in Fig. 8, where the ratio of switching power P_{sw} to the stationary power $P_0 = |g_1^{st}|^2$ of the slave laser is plotted as a function of $\Delta\omega$. Yet, if $\Delta\omega \simeq 1$ the switching power P_{sw} is still low: for instance, in the case of Fig. 7, $\Delta\omega = 3$, $P_{sw} \simeq 0.15\,P_0$ and the other parameters which determine the total energy according to Eq. (3.2) are $\sigma = 6$ and $\tau_r = 0.2 \times 10^{-9}$ s. Then, assuming $P_0 = 0.1$ mW, the switching energy is $E_{sw} = \sigma\tau_r P_{sw} \simeq 20$ fJ.

IV. LOGIC GATES

Having demonstrated the feasibility of optical switching between modes TEM_{10} and TEM_{01} in a VCSEL with square-shaped active region, we are now ready to apply this result to the realization of optical logic gates.

The logic gates most commonly used are the NOT, the OR, the AND, the NOR and the NAND. Among these only the NOR and the NAND are fundamental, in the sense that combining a certain number of NOR or NAND gates it is possible to build any other logic gate.

A NOR gate can be realized as follows: two input beams (I_1, I_2) are injected in correspondence with the two peaks of one mode, say mode TEM_{01} ; the detector which measures the output (O) and a reset beam (Re) are placed on the other diagonal of the square (Fig. 9). Both the individual input beams and the reset beam have sufficient intensity to cause switching from one to the other mode.

We assign the value "1" to each of the inputs I_1 and I_2 when they are "on" and "0" when they are "off". The detector measures "0" (no intensity) if the laser emits mode TEM_{01} and

"1" (finite intensity) if the laser emits mode TEM_{10} . The reset beam, which is injected at the beginning of each operation, is necessary to ensure that initially the laser emits mode TEM_{10} . Then, if no beam is sent to any of the two inputs (i.e. $I_1 = I_2 =$ "0") the output is "1"; in all other cases the laser switches to mode 0 and the output is "0"; hence the system works as a NOR gate.

Fig. 10 shows the time evolution of mode intensities in the case in which both input beams take the value "1". The solid line represents mode TEM_{10} and the dashed line represents mode TEM_{01} . The whole operation consists of various steps.

a) the reset beam is switched on (in this particular case we assume that the result of the previous operation was "0", that is the laser was on mode TEM_{01})

b) the reset beam is switched off and the laser reaches the TEM_{10} mode

c) the two input beams are injected, one after the other, into the laser

d) the injection of the input beams causes the switching to mode TEM_{01}

e) the output is detected

In step c) the time separation between the injected pulses, of about 3 times their duration, is necessary to avoid any interference between them, that in special cases might destroy the switching. The whole logic process a)-e) takes about $150\tau_r$.

An OR gate is immediately obtained from the NOR simply by locating the output in the other diagonal; a NOT gate can also be obtained from the NOR one, by simply eliminating one of the input signals.

For the AND and NAND gates the situation is more complicated, because the laser must switch only when both input beams are "on". One can think of injecting simultaneously the two beams, setting the intensity of the "on" signal to a value in the range between the switching threshold and one half of it; unfortunately the two pulses, depending on their detuning and phase difference, can interfere and cancel each other. It becomes therefore necessary to control the interference conditions or change globally the whole device design: investigation are going on in both these directions.

We observe that the scheme proposed here for logic gates can work only when the two stable states of the laser do not overlap in the transverse plane, as in the case of modes TEM_{10} and TEM_{01} . In this way the two output levels are associated with two intensity levels of the emitted field in a particular point.

The situation in which the two bistable states are the doughnut modes is less convenient for applications, because in this case the two outputs have the same intensity levels and they can be discriminated only by means of phase-sensitive techniques [6].

We note also that the kind of logic gate we propose has gain, and therefore allows for cascadability.

V. CONCLUSIONS

We have demonstrated that VCSELs possess an especially interesting feature with respect to other kinds of lasers: the two Gauss–Hermite modes TEM_{10} and TEM_{01} are both stable with an appropriate choice of the parameters and geometry. This property of VCSELs is the basis for applications to optical switching and logic gates.

Yet, the realization of physical devices will be possible only when some practical problems will be solved. First of all, the VCSELs must have a large degree of transverse homogeneity in order to have frequency degeneracy between the two modes. Asymmetries or strains of the material can break the frequency degeneracy, and make bistability impossible [8]. We are confident that in a reasonable time VCSELs with a sufficient degree of homogeneity will be available.

Another difficulty is represented by the necessity of focussing the injected beam to a size on the order of a few microns, in order to excite only the desired mode. Spatial drifts of the injected field could also be detrimental for the reliability of the device.

From the point of view of the theoretical model, a more realistic description should include grating effects and diffusion, and we are working in this direction.

In any case VCSELs, because of their particular properties, seem to be interesting best candidates for applications to information processing.

ACKNOWLEDGMENTS

We thank Prof. J. McInerney and Dr. Hua Li for very helpful and stimulating discussions, and for disclosing us their experimental results before publication. Work in the framework of the ESPRIT BR Project 7118 TONICS and of the NATO Collaborative Research Grant 921142.

REFERENCES

[1] L. A. Lugiato, Phys. Rep. **219**, 293-310 (1992)

[2] C. O. Weiss, Phys. Rep. **219**, 311-328 (1992)

[3] M. Brambilla, F. Battipede, L. A. Lugiato, V. Penna, F. Prati, C. Tamm and C. O. Weiss, Phys. Rev. A **43**, 5090-5113 (1991)

[4] M. Brambilla, L. A. Lugiato, V. Penna, F. Prati, C. Tamm and C. O. Weiss, Phys. Rev. A **43**, 5114-5120 (1991)

[5] C. Tamm, Phys. Rev. A **38**, 5960 (1988)

[6] C. P. Smith, Y. Dihardja, C. O. Weiss, L. A. Lugiato, F. Prati and P. Vanotti, Opt. Commun. **102**, 505-514 (1993)

[7] J. L. Jewell, J. P. Harbison, A. Scherer, Y. H. Lee and L. T. Florez, IEEE Journal of Quantum Electronics **27**, 1332-1346 (1991)

[8] H. Li, T. L. Lucas, J. McInerney and R. A. Morgan, *Transverse Modes and Patterns of Electrically Pumped Vertical Cavity Surface Emitting Semiconductor Lasers*, Chaos, Solitons and Fractals, special issue entitled Nonlinear Optical Patterns, Structures and Chaos, to appear

[9] C. H. Henry, IEEE Journal of Quantum Electronics **QE-18**, 259-264 (1982)

[10] F. Prati, A. Tesei, L.A. Lugiato and R.J. Horowicz, *Stable States in Surface-emitting Semiconductor Lasers* Chaos, Solitons and Fractals, special issue entitled Nonlinear Optical Patterns, Structures and Chaos, to appear

[11] F. Prati, M. Brambilla and L. A. Lugiato, La Rivista del Nuovo Cimento, Vol. 17, n. 3 (1994)

[12] E. J. D'Angelo, E. Izaguirre, G. B. Mindlin, G. Huyet, L. Gil and J. R. Tredicce, Phys. Rev. Lett. **68**, 3702 (1992)

Figure captions

Fig. 1 Schematic representation of the laser. a) Lateral view, b) top view. R is the mirror reflectivity, l and L_A are the transverse and longitudinal dimensions of the active region, respectively.

Fig. 2 Intensity distribution of the doughnut, TEM_{10} and TEM_{01} laser modes in the transverse plane. The square represents the transverse section of the active region.

Fig. 3 Stability domains of the solutions $A_{0,\pm1}$, TEM_{10} and TEM_{01} in the plane (ψ,β). The dashed line represents the laser threshold.

Fig. 4 Undamped oscillations of the TEM_{10} and TEM_{01} modes under injection of a high energy pulse with $P = 0.15\,P_0$, and $\sigma = 50$. The other parameters are $\beta = 0.032$, $\tilde{k} = 10$, $\alpha = 4$ and $\psi = 2$.

Fig. 5 Behaviour of the laser modes amplitudes upon injection of a low energy pulse with $P = 0.0005\,P_0$ and $\sigma = 2$; a phase difference of 135 degrees is assumed between the injected pulse and the initial stationary cavity field. In a) and b) are shown respectively the mode amplitudes as a function of time and their evolution in the complex plane: switching takes place.

Fig. 6 Behaviour of the laser modes amplitudes upon injection of a low energy pulse with $P = 0.0005\,P_0$ and $\sigma = 2$; a phase difference of 180 degrees is assumed between the injected pulse and the initial stationary cavity field. In a) and b) are shown respectively the mode amplitudes as a function of time and their evolution in the complex plane: the switching does not take place.

Fig. 7 Behaviour of the laser mode amplitudes upon injection of a pulse with $P = 0.15\,P_0$ and $\sigma = 6$; a detuning $\Delta\omega = 3$ is assumed between the injected and the laser field.

Fig. 8 Variation of the laser switching threshold P/P_0 with increasing detuning, for an injected pulse with $\sigma = 6$.

Fig. 9 Scheme of the logic gate NOR. I_1 and I_2 are the input beams, O is the output and Re is the reset beam.

Fig. 10 Time behaviour of the laser mode amplitudes during the sequence a)-e) described in the text, with the input beams assumed to be both "on"; the solid line represents mode TEM_{10} (reset beam and output) and the dashed line represents mode TEM_{01} (input beams).

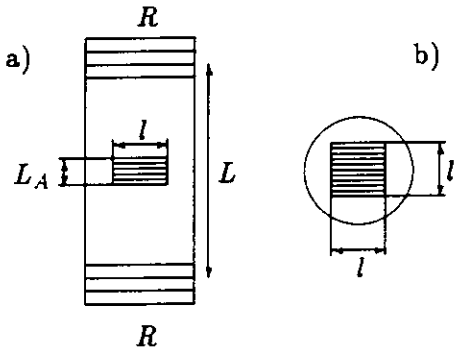

Fig. 1

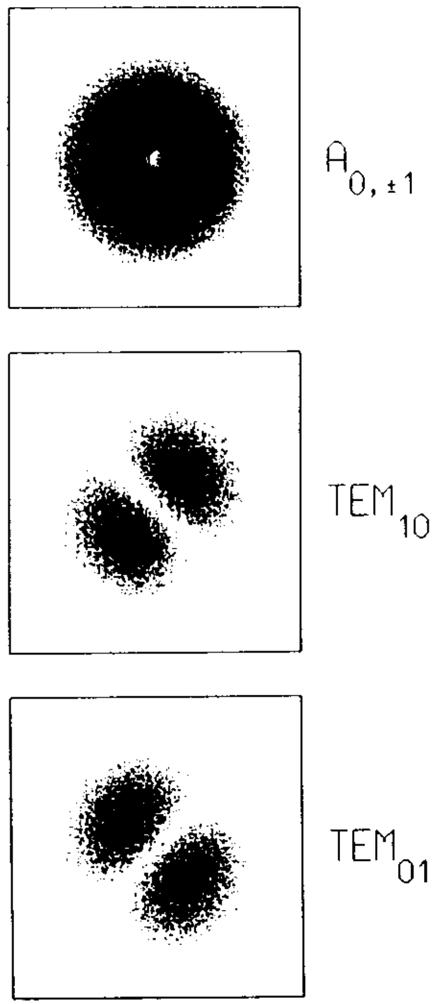

$A_{0,\pm1}$
TEM_{10}
TEM_{01}

Fig. 3

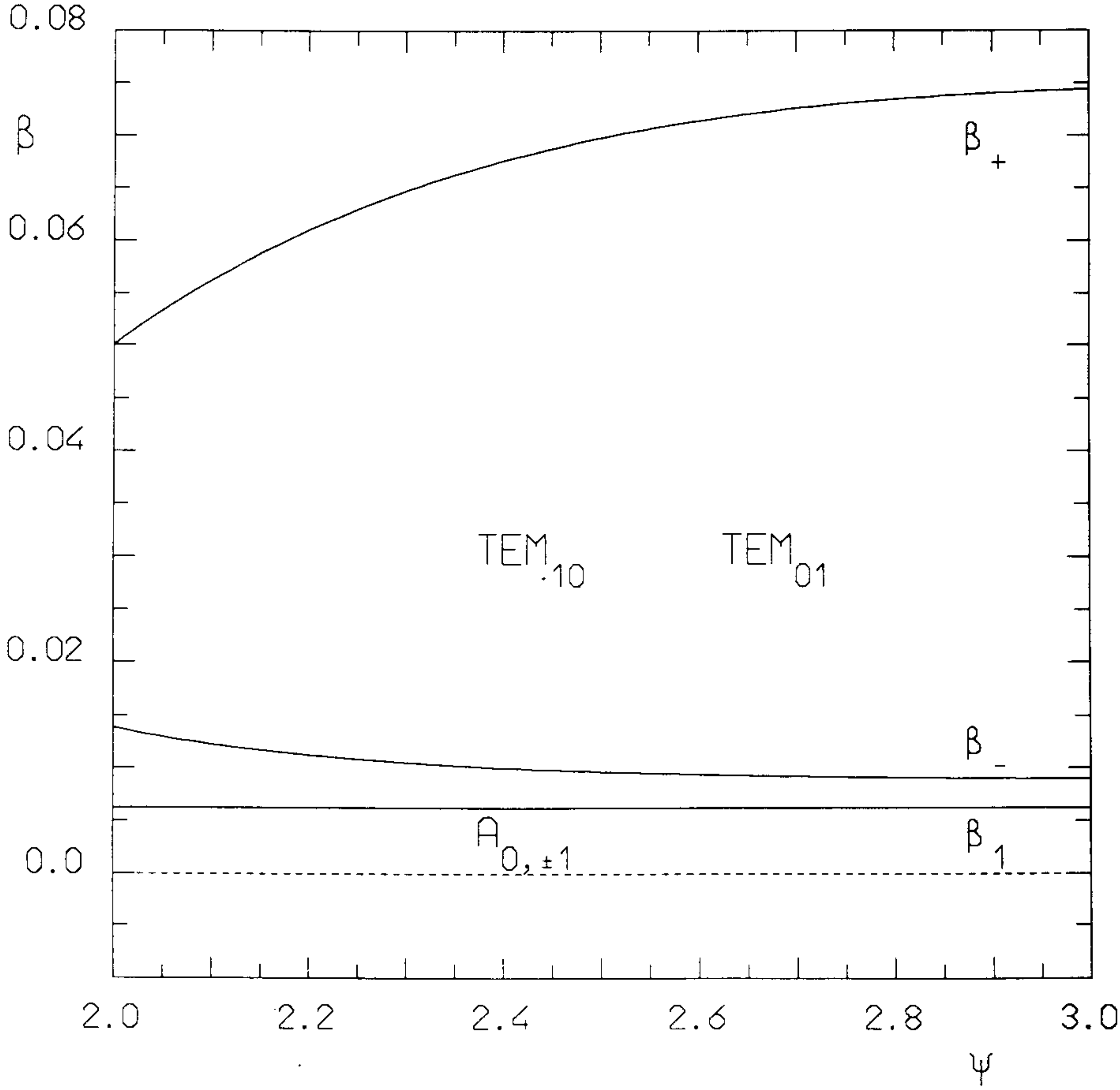

Fig 4

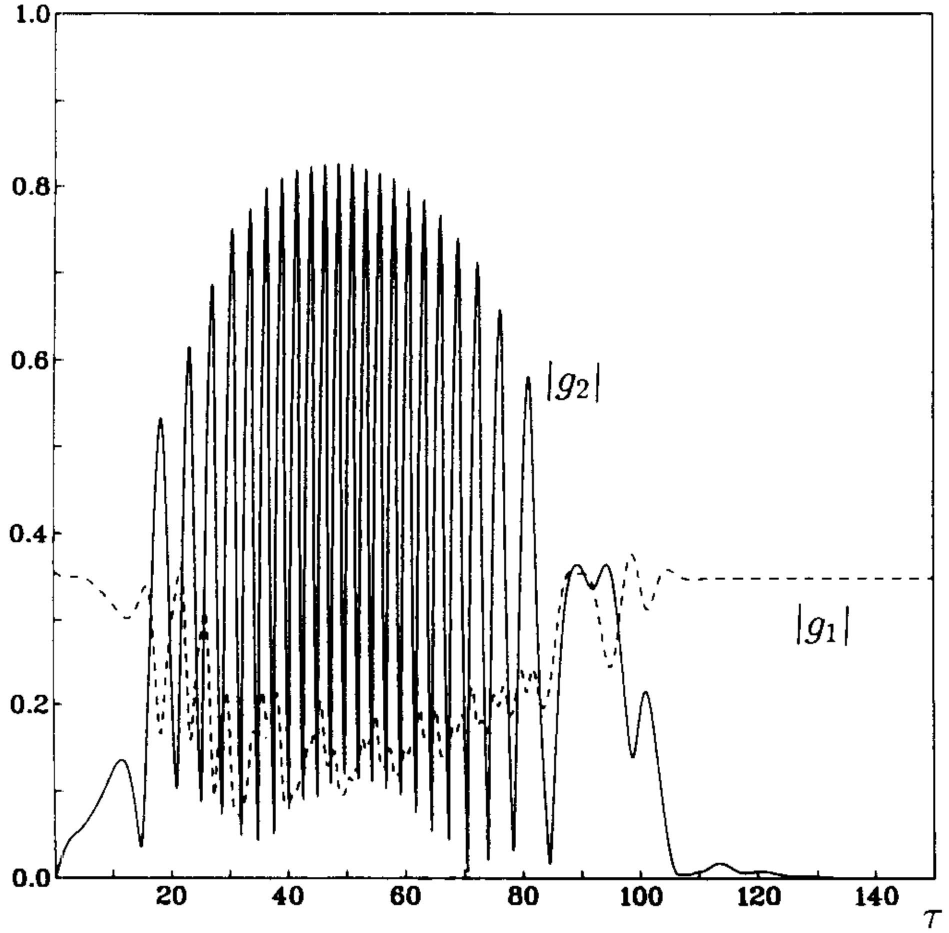

AG

Fig. 5

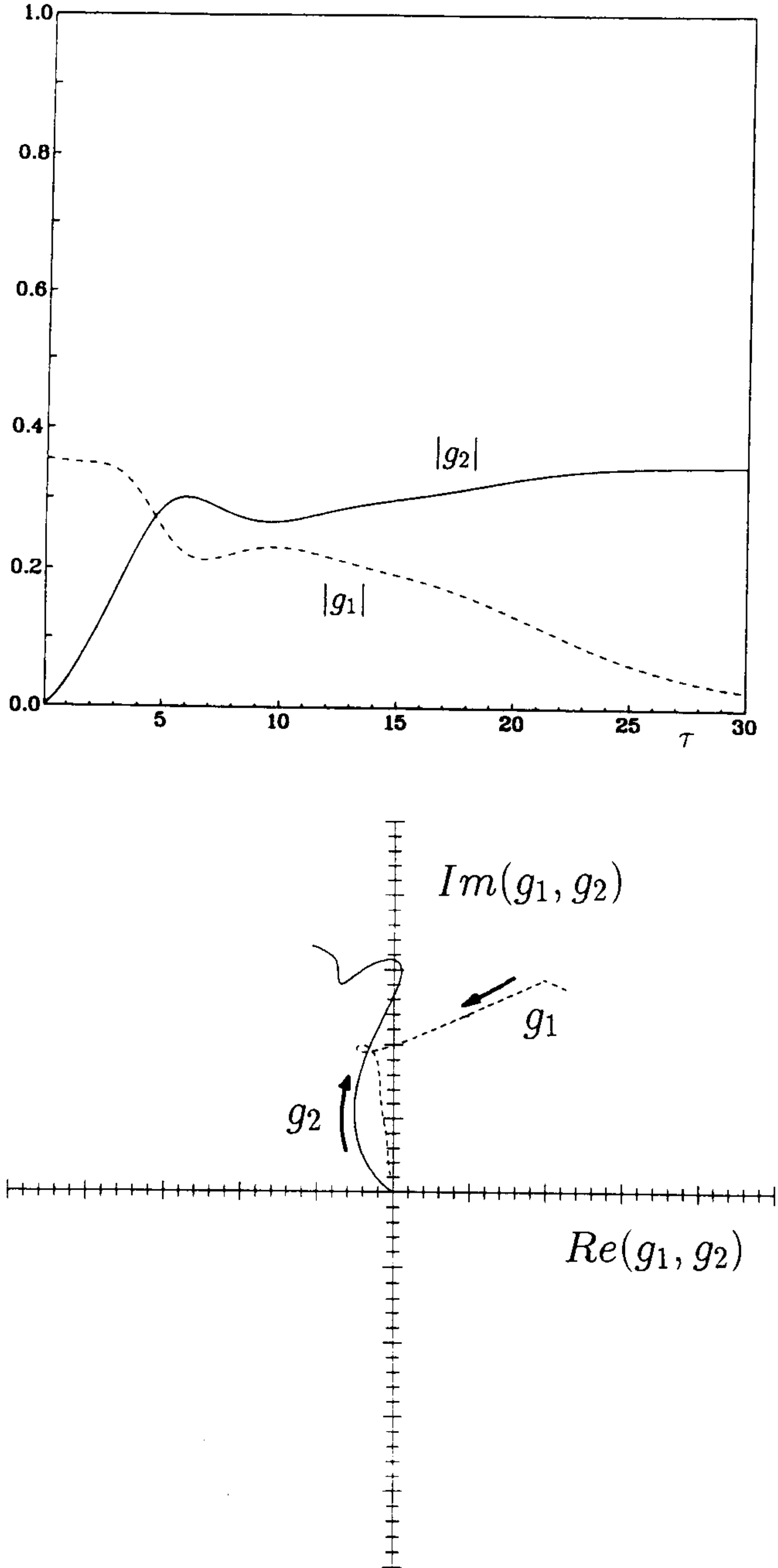

Fig 6

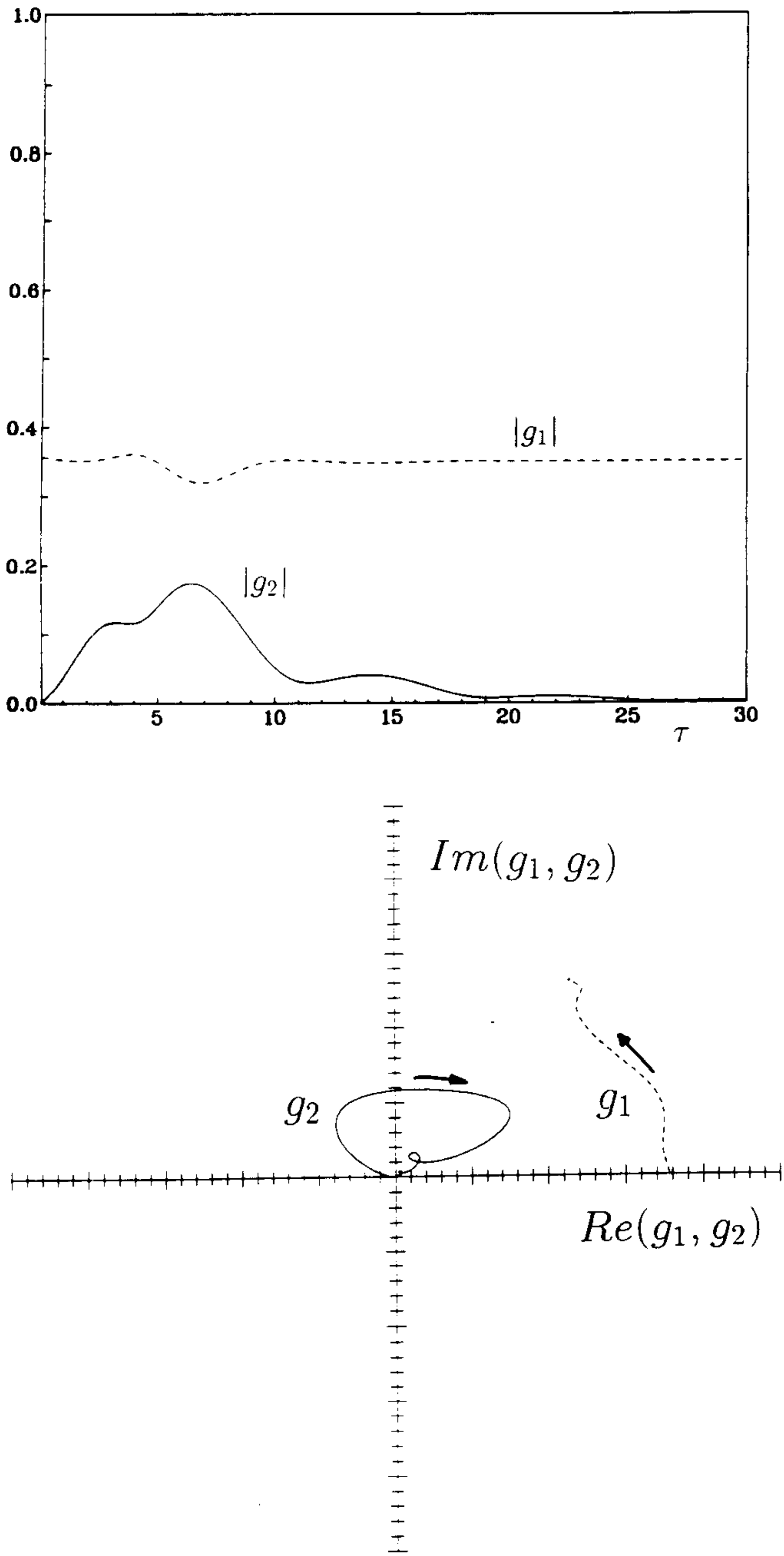

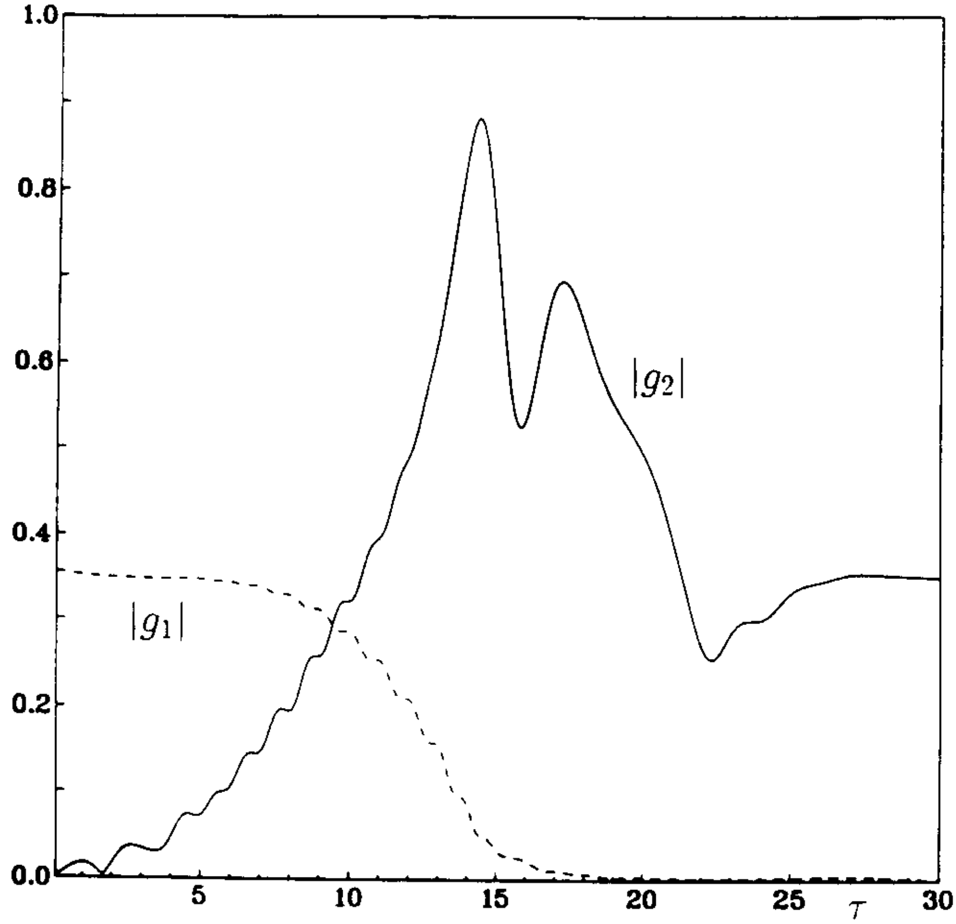
1.0
0.8
0.6
0.4
0.2
0.0
5
10
15
20
25
30
τ
|g2|
|g1|

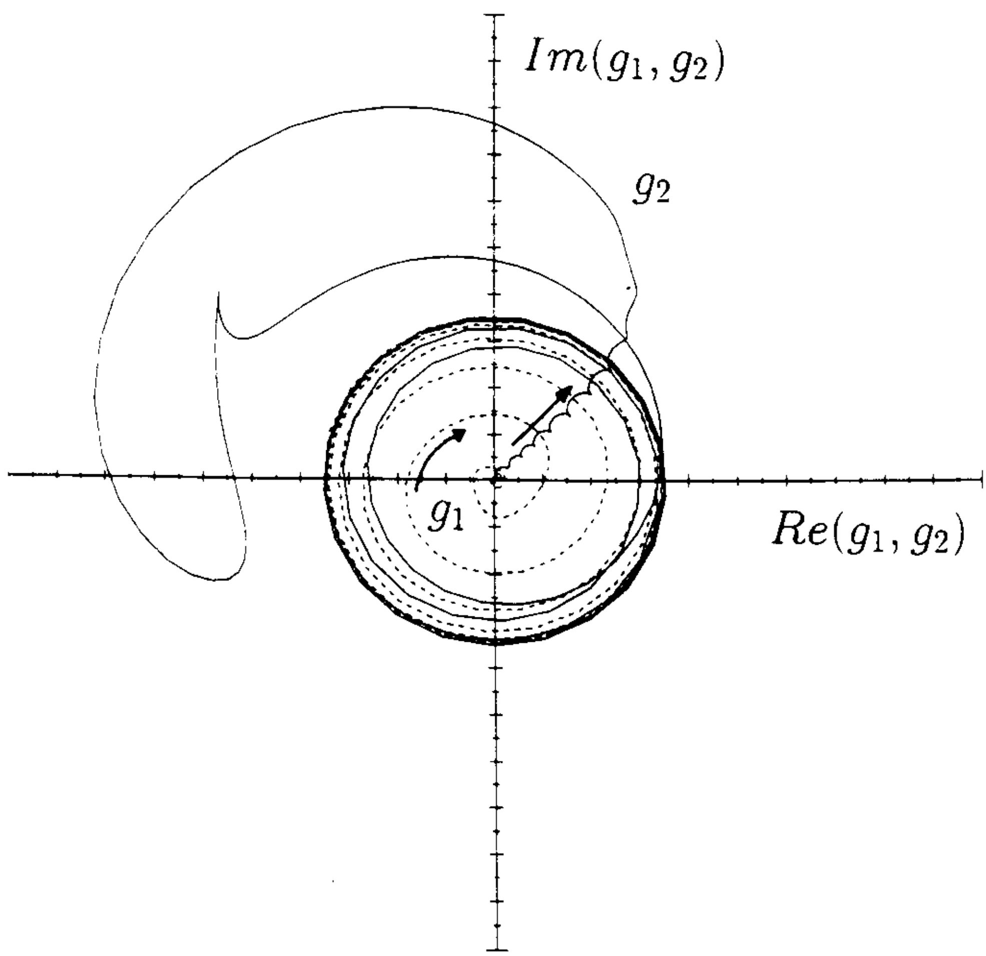
Im(g1, g2)
Re(g1, g2)
g2
g1

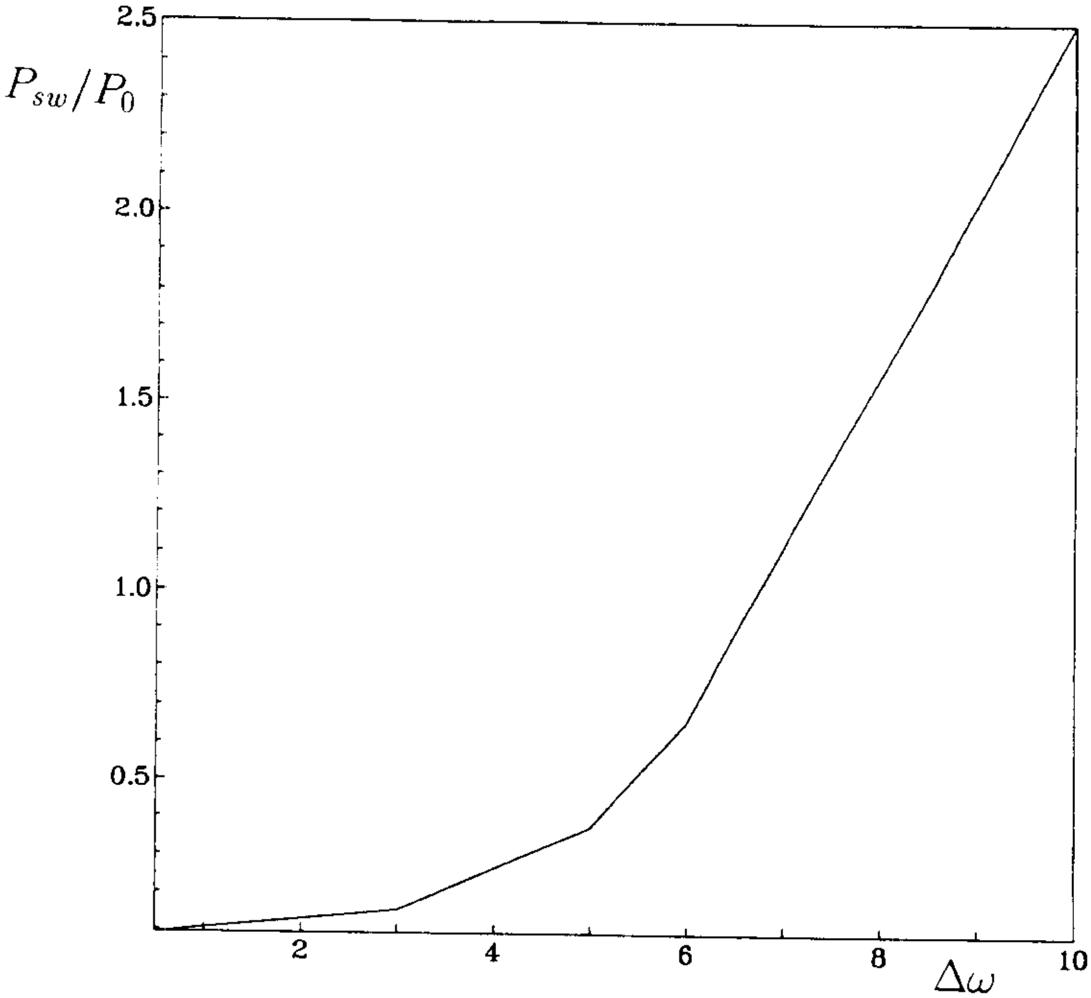

Fig. 5

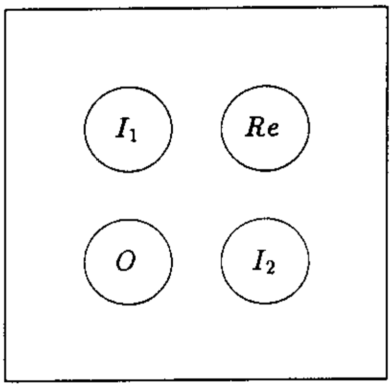

Fig 9

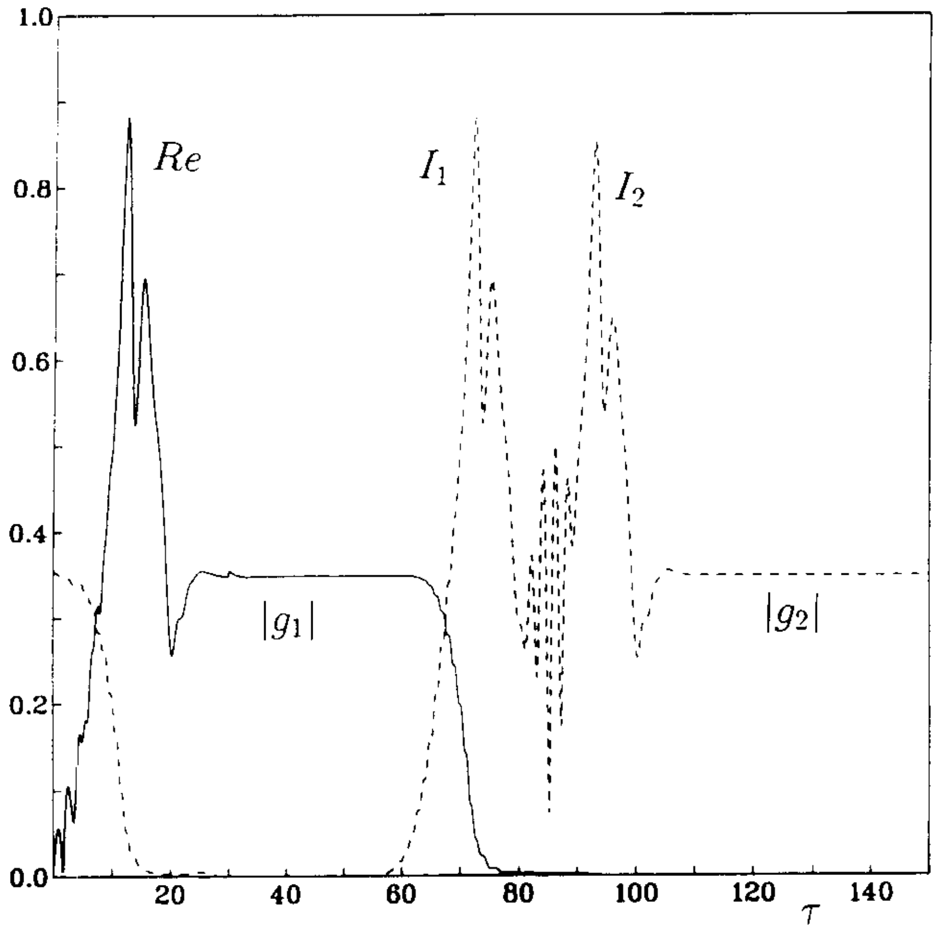

1.0
0.8
0.6
0.4
0.2
0.0
20
40
60
80
100
120
140
τ
Re
I_1
I_2
$|g_1|$
$|g_2|$